Published in final edited form as:
Proteomics. 2008 November ; 8(22): 4695–4708. doi:10.1002/pmic.200700596.

PTP-ε HAS A CRITICAL ROLE IN SIGNALING TRANSDUCTION PATHWAYS AND PHOSPHOPROTEIN NETWORK TOPOLOGY IN RED CELLS

Lucia De Franceschi[1], **Andrea Biondani**[1], **Franco Carta**[2], **Franco Turrini**[3], **Carlo Laudanna**[4], **Renzo Deana**[5], **Anna Maria Brunati**[5], **Loris Turretta**[5], **Achille Iolascon**[6], **Silverio Perrotta**[7], **Ari Elson**[8], **Cristina Bulato**[5], and **Carlo Brugnara**[9]

[1]Dept of Clinical and Experimental Medicine, Section of Internal Medicine, University of Verona, Verona, Italy

[2]Porto Conte Ricerche, Alghero, Sassari, Italy

[3]Dept of Biochemistry, University of Torino, Torino, Italy

[4]Dept of Pathology, Section of General Pathology, and CMC-Center for Biomedical Computing, University of Verona; Italy

[5]Dept of Biochemistry, University of Padova, Padova, Italy

[6]Chair of Medical Genetics, Department of Biochemistry and Biotechnologies, University Federico II -GEINGE, II Advanced Biotechnologies, Napoli, Italy

[7]Dept of Pediatrics, II University of Napoli, Napoli, Italy

[8]Molecular Genetics, Weizmann Institute of Science, Rehovot, Israel

[9]Depts of Pathology and of Laboratory of Medicine, Children's Hospital, Harvard Medical School, Boston, MA, USA

Abstract

Protein tyrosine phosphatases (PTPs) are crucial components of cellular signal transduction pathways. We report here that red blood cells (RBCs) from mice lacking PTPε (Ptpre$^{-/-}$) exhibit abnormal morphology and increased Ca^{2+}-activated-K^+ channel activity, which was partially blocked by the Src-Family-Kinases (SFKs) inhibitor PP1. In Ptpre$^{-/-}$ mouse RBCs, the activity of Fyn and Yes, two SFKs, were increased, suggesting a functional relationship between SFKs, PTPε and Ca^{2+}-activated-K^+-channel. The absence of PTPε markedly affected the RBC membrane tyrosine (Tyr-) phosphoproteome, indicating a perturbation of RBCs signal transduction pathways. Using signaling network computational analysis of the Tyr-phosphoproteomic data, we identified 7 topological clusters. We studied cluster 1, containing Syk-Tyr-kinase: Syk-kinase activity was higher in wild-type than in Ptpre$^{-/-}$ RBCs, validating the network computational analysis and indicating a novel signaling pathway, which involves Fyn and Syk in regulation of red cell morphology.

Keywords

Tyrosine-phosphorylation; Fyn; Syk; Gardos channel

Corresponding author: Lucia De Franceschi, MD, Department of Clinical and Experimental Medicine, Section of Internal Medicine, University of Verona, Policlinico GB Rossi; P.le L Scuro, 10; 37134 Verona, Italy phone: +390458074918; FAX: +39045580111; lucia.defranceschi@univr.it.

1. INTRODUCTION

Protein tyrosine phosphatases (PTPs) are crucial components of signal transduction pathways in different cell types [1–4]. The balance between the competing activities of protein tyrosine phosphatases and protein-tyrosine-kinases (PTKs) is responsible for changes in protein tyrosine phosphorylation and function [2,3,5,6]. Studies with inhibitors of PTPs, such as vanadate, have shown that PTPs are important regulators of cell differentiation in several cell lines [3]. In human red cells, vanadate appears to block Ca^{2+} pumps [7] and to modulate the tyrosine phosphorylation of several membrane proteins [4,8–10]. Although information on PTPs function has been obtained with the use of general inhibitors of PTPs [10–12], the presence of specific PTPs in red cells, their role in erythrocyte signal transduction pathways and their activities have not been fully explored.

Recently, mouse models lacking protein tyrosine phosphatase epsilon (PTPε) have been developed. PTPε knockout mice ($Ptpre^{-/-}$) show: (i) hypomyelination of sciatic nerve axons at early post-natal age correlating with increased activity of delayed-rectifier-voltage-gated-K^+ channel in Schwann-cells; (ii) abnormalities in macrophage functions; (iii) defects in osteoclast subcellular organization and cellular activities; and (iv) reduction in the extent of transformation in Neu-induced mammary tumors [13–16].

The PTPε phosphatase subfamily contains four distinct proteins generated by a single gene. The receptor-type (RPTPe) and the non-receptor-type (cyt-PTPe) are the two more abundant PTPε isoforms in cells and differences in their amino termini result in distinct functions [2,17,18]. Recent studies have shown that PTPε isoforms regulate a number of intracellular pathways including: the activity of specific kinases such as MAP-kinase [19], JAK-STAT signaling pathway in M1-leukemia cells [1] and c-Src [16] in various cell types.

Here, we show that PTPε is expressed in mouse erythrocytes and is involved in red cell signaling networks. We found that mouse red cells lacking PTPε have abnormal morphology, reduced intracellular K^+ content and increased Ca^{2+} activated-K^+ (Gardos) channel activity and that cell dehydration can be reversed *in vivo* with the use of the Gardos channel inhibitor clotrimazole. We report that the Gardos channel activity is partially blocked by the Src-Family Kinase (SFK) inhibitor PP1, and that the activity of Fyn, a SFK, is increased in mouse red cells lacking PTPε compared to wild-type, suggesting a functional relation between SFKs and Gardos channel activity. We also demonstrate that the red cell membrane tyrosine phosphoproteome of the $Ptpre^{-/-}$ mice differs from that observed in wild-type mice, reflecting perturbation of cell signaling networks.

2. MATERIALS AND METHODS

Mice

Gene-targeted mice lacking PTPε ($Ptpre^{-/-}$ mice, C57BL/6 × 129 genetic background) [13] were handled according to the Institutional and National guidelines for the care and use of laboratory animals. Macroscopic and microscopic feature of liver or spleen were not different in $Ptpre^{-/-}$ compared to wild-type mice (data not shown).

Hematological parameters and red cell morphology

Blood was collected from isofluorane-anesthetized mice and immediately used for ion transport fluxes and/or Ca^{2+} activated-K^+ channel measurements, determination of red cells density profiles, cell morphology and hematological parameters. Hematocrit (Hct) was determined by centrifugation in a micro-Hct centrifuge. Erythrocyte and reticulocyte cellular indices were determined on an ADVIA 120 hematology analyzer, using a mouse-specific

software program (Siemens Medical Solutions Diagnostics, Tarrytown, NY). [20,21] RBCs density distribution curves were obtained using phthalate esters in microhematocrit tubes as previously reported; the density values defined as the 20% densest fraction of RBCs (D_{20}) were determined for each curve [22–24].

RBC ghosts were prepared and RBC membrane protein expression was analysed by sodium dodecyl sulfate-polyacrylamide gel electrophoresis as previously reported [25–27]. The content of spectrin dimers and tetramers was determined by nondenaturing gel electrophoresis. The percentage of RBCs exposing phosphatidyl-serine (PS) was assessed with Annexin-V labeling as previously described [28].

Red cell cation content, membrane cation transports and Ca^{2+} activated-K^+ channel activity

Erythrocyte Na^+ and K^+ content was determined in washed red cells as previously described [29]. RBC calcium ion concentration ($[Ca^{2+}]_c$) was measured according to Lidner et al. [30] RBC calcium ion concentration ($[Ca^{2+}]_c$) was measured according to Lidner et al.. Fluo-3 probe was chosen because of its spectral characteristics that are indicated for determination of $[Ca^{2+}]_c$ in red cell. The suspension was supplemented with 5% bovine serum albumin and erythrocytes were separated by centrifugation (10 min at 500 *g*) and resuspended in the above medium (about 2×10^6/ mL) supplemented with 0.5 mM $CaCl_2$. Fluorescence was measured at 37°C in a thermostated, magnetically stirred cuvette adopting excitation and emission wavelengths of 506 and 526 mm respectively. The calibration was performed by adding in sequence calcium ionophore ionomycin, detergent digitonin, calcium chelator EGTA and Co^{2+}. The buffer contaminating Ca^{2+} was determined by means of Arsenazo III [30–32].

Maximal rate for Na/K pump, Na/K/2Cl cotransport and K/Cl cotransport were measured in wild-type and $Ptpre^{-/-}$ mouse red cells as previously described [23,24]. Nominal maximal activity of the Ca^{2+}activated-K^+ channel was measured as Rb^+ influx stimulated by ionophore A21387 (80 μM) in washed RBCs in the presence of 50 μM $CaCl_2$ [29]. Whenever indicated the experiments were carried out in presence of either the protein kinase C inhibitor, Calphostin C (1 μM) [33,34] or the Src-family kinases inhibitor PP1 (10 μM). [5,35] For channel kinetic analysis, the charybdotoxin (ChTX)–sensitive K^+ influx was calculated from total Rb^+ influx in the presence of 50 nM ChTX.[29] Free ionic calcium was buffered with 1 mM EGTA (ethyleneglycotetraacetic acid) or citrate buffer as previously described [22]. Extracellular dissociation constant was calculated by using the dissociation constant (K_d) for EGTA or citrate and correcting for ionic strength at pH 7.4 and 0.15 mM $MgCl_2$ as previously described [22].

In vivo Gardos channel inhibition by Clotrimazole (CLT)

$Ptpre^{-/-}$ and wild-type mice were divided into 2 groups of 6 animals each which were either treated with vehicle or CLT (160 mg/Kg twice a day) administrated by gavage [22,36]. Hematological parameters, phthalate RBC density population curves and RBC cation content were evaluated at baseline and after 12 days of treatment. Mice from both strains were alive and well at the end of the treatment.

PTPε protein expression, Fyn, Hck, Syk kinase expression and activity

Mouse packed RBCs were lysed in ice cold Phosphate Lysis Buffer (LB: 5 mM Na_2HPO_4 pH 8.0, containing: protease inhibitor cocktail tablets (Roche), 3 mM benzamidine, final concentration), and centrifuged 10 min at 4°C at 12,000 × *g*. RBCs ghosts were washed several times in LB. Ghost protein content was quantified using DC Protein Assay (Biorad), separated by electrophoresis and blotted with polyclonal anti-PTPε antibody. We used

extracts of HEK293 cells transiently over-expressing cytoplasmatic-PTPε and receptor-PTPε protein as positive controls [17,18]; while anti-actin (Sigma Chemical Co, St Louis, MO) was used as loading control. Expression of Hck, Fyn, Yes and Syk was evaluated by immunoblotting analysis using specific anti-Hck (N30-clone, SantaCruz Biotechnology, CA, USA), anti-Fyn (FYN3; SantaCruz Biotechnology, CA, USA), anti-Yes (Clone 3 SantaCruz Biotechnology, CA, USA) anti-Syk antibody (Cell Signaling Technology, Inc, CA, USA). The activity of Hck, Fyn, Yes and Syk was measured by in vitro kinase assays on specific immunoprecipitates from erythrocyte lysates for Hck, Fyn, Yes and Syk and from red cell ghosts for Syk as previously described [23]. The Fyn kinase activity as phosphorylation of Tyr residues of target proteins, was monitored by supplementing an exogenous substrate, enolase, to the reaction mixture, as previously described [37]. The Syk kinase activity as phosphorylation of Tyr residues was evaluated on endogenous substrates: band 3 and synuclein [35,38]. Syk immunoprecipitated from erythrocyte lysates were incubated in 30 μl mixture containing 50 mM Tris-HCl, pH 7.5; 10 mM $MnCl_2$, 10 μM γ [^{32}P] ATP (specific activity 1000 cpm/pmol), 100 μM sodium orthovanadate (basal medium), and either band 3 (6 μg red cells ghosts) or synuclein (0.5 μg) [35,38]. Following incubation for 10 min at 30° C, samples were resolved on SDS-PAGE (11% gels) transferred to nitrocellulose membranes. The blots were probed with anti-Syk antibody as loading control. Syk kinase activity was visualized by autoradiography of blots.

Red cell membrane protein tyrosine phosphorylation pattern and identification

RBC ghosts were solubilized for either one-dimensional (1D) or two-dimensional electrophoresis (2D). For 2Ds, RBC ghost proteins were extracted with 7M urea, 2M thiourea, 2% CHAPS, 2% TRITON X-100, 1% DTT solution and 2.5 % Ampholine. 2-DEs were performed using a IPGphor system (Amersham Biosciences, Uppsala, Sweden) for the first dimension and the Ettan Dalt Six (Amersham Biosciences) for the second dimension. Samples were in gel-rehydrated (24 hs RT) and run on 7 cm, pH 4–7 IPG strips (4% T, 3% C, Amersham Bioscience). Total voltage applied was 60,000 V/h. After equilibration, the strips were run in the second dimension on to Ettan Dalt Six. 1D and 2D gels were run in duplicate; one gel was subsequently stained with colloidal Coomassie and the other one was used for Western-blot analysis with specific anti-phosphotyrosine antibodies (PY99-clone SantaCruz Biotechnology, CA, and 4G10-clone, UpState, NY, USA). The bands or the spots differently phosphorylated were identified by image gel analysis, using Image Master 2D Platinum software, version 5.0 (GE Healthcare, Little Chalfont, UK) by desnitometric analysis of the scanned images of unsaturated films (ImageJ v 1.28 software). The selected bands or spots were identified by MALDI-TOF MS/MS analysis. In some studies, Tyr-phospho-enriched membrane proteins immunoprecipitates were solubilized, separated by 1-DE and colloidal Coomassie stained for MALDI-TOF MS/MS analysis.

MALDI-TOF MS analysis and Database search—Mass spectrometric analyses was performed using a Tofspec SE (Micromass, Manchester, UK). Peptide spectra were obtained in positive ion mode over the m/z range of 800 – 4000 Da range or 1000–3000 Da in reflectron mode. Peptide solution was prepared mixing equal volumes of matrix (matrix: saturated a-cyano-4-hydroxy cynnamic acid solution in 40% acetonitrile, 60% of 0.1% trifluor acetic acid). 100 – 120 laser shots were summed for each MS spectrum. Database searching was performed using the measured peptide masses against the Swiss-Prot database (*taxa Rodentia*) using the MASCOT search engine (Matrix Science Ltd, London, UK) Only protein identifications with significant Mascot score ($p < 0.05$) were taken in consideration. A mass accuracy of 0.3 Da and a single missed cleavage were allowed for each matching peptide. Searches were not constrained by pI or molecular weight. The sites of phosphorylation have been confirmed by demonstraton of mass shift of the peptides following phosphatase treatment as previously described by Torres et al. [39].

Phosphoproteomic network computational analysis

A Global Network, including about 18,700 proteins and 42,500, non-redundant, binary interactions was generated by combining the data-sets from HPRD, BIND, DIP and MINT protein interaction data-bases. The Global Network includes only mammalian protein-protein interactions (78% human, 16% mouse and 6% rat). Only manually curated, experimentally determined, protein-protein interactions were included. We did not consider interactions derived only from two-hybrid analysis, not validated by other methods. The data set was compiled in Cytoscape (.sif) or in VisAnt (.txt) formats. The analysis was performed with Cytoscape ver. 2.2 [40] (sub-network reconstruction, modular decomposition with the MCODE algorithm [41] and GO analysis) or with VisAnt ver 2.4[42] (global topological analysis). Both the packages were open source and freely available from www.cytoscape.org and from visant.bu.edu. The analysis of Gene Ontology was performed by BINGO Cytoscape plug-in [43]. Protein annotation data were obtained from www.gopubmed.org, www.geneontology.org and from www.cellmigration.org.

Statistical analysis

Data were treated by the 2-way ANOVA algorithm for repeated measurements. Differences with $p<0.05$ were considered significant. Data are reported as the means ± SD.

3. RESULTS

Mice lacking PTPε show red cells with abnormal morphology and density profile

Gene-targeted mice lacking PTPε ($Ptpre^{-/-}$) showed abnormal red cell morphology, with micro-spherocytic, acanthocytic, and fragmented erythrocytes (Fig. 1a, b). In order to characterize the red cell features of $Ptpre^{-/-}$ mice, we first verified whether PTPε protein was expressed in mouse red cells. The receptor form of PTPε (RPTPε) was present in wild-type mouse red cell membrane, whereas it was almost undetectable in red cells membrane from the knockout mice ($Ptpre^{-/-}$). In contrast, the nonreceptor form of PTPε (cyt-PTPε), which is generally found in the cell cytoplasm, was undetectable in both normal and knockout mouse red cells (data not shown). This last result is consistent with previous studies, which indicated that RPTPe and cyt-PTPe are not expressed in the same cell type [19]. Since the antibodies used for blotting experiments cross-react with RPTPα protein, we detected the presence of RPTPα in both mouse strains, with no differences in its abundance between wild-type and knockout mouse red cells (Fig. 1c).

Mice lacking PTPε exhibited red cell dehydration as indicated by the rightward shifting in the red cell corpuscular hemoglobin (Hb) distribution with corresponding increase in mean cell hemoglobin concentration (MCHC; Table 1, Fig. 1b) and the presence of denser cells on the phthalate density profile (wild-type D_{20}: 1,090±0,002 *vs* $Ptpre^{-/-}$ D_{20}: 1,096±0,001, n= 9; $P<0.05$). Although the reticulocyte count was similar in wild-type and knockout mice, the increase in MCHCr and the reduction in RDWr suggest that fragmentation and dehydration are present at the reticulocyte stage as well (Table 1).

In $Ptpre^{-/-}$ mouse red cells, the osmotic fragility curves show a trend towards higher fragility values compared to control erythrocytes, without reaching statistical significant differences except for one point at 160 mOsm (Fig. 2a; $P<0.05$, n=10), suggesting that the dehydration may be accompanied by a reduction in surface area of the cell membrane, as seen in some cytoskeletal hereditary red cell disorders [22]. $Ptpre^{-/-}$ red cells show a marked decrease in red cell K^+ content, without significant changes in red cell Na^+ content compared to normal erythrocytes (Table 1).

We asked next whether the absence of PTPε could affect red cell membrane protein composition, which was similar in both mouse strains (data not shown).

Since optimal red cell morphology also depends on the maintenance of membrane phospholipid asymmetry, we evaluated the percentage of red cells exposing phosphatidylserine (PS) on the surface of plasma membranes [44]. Using Annexin-V binding to detect PS externalization [45], we observed no significant differences in the percentage of PS-exposing red cells in Ptpre$^{-/-}$ mice compared to controls, suggesting that the absence of PTPε did not markedly affect the lipid-lipid and lipid-protein interactions (Table 1).

The Ca^{2+} activated K^+ channel activity is abnormally regulated in Ptpre$^{-/-}$ mouse red cells

To investigate the mechanisms involved in generation of dense red cells in mice lacking PTPε, we evaluated the activity of the main cation transport systems and the Ca^{2+}activated-K^+ channel in red cells from both mouse strains. The absence of PTPε did not modify the activities of the Na/K pump and of the Na/K/2Cl cotransport, while the activity of K/Cl cotransport (KCC) was slightly but not statistically significantly higher in Ptpre$^{-/-}$ red cells than in wild-type erythrocytes (Fig. 2b). To properly characterize the activity of the Gardos channel, we first evaluated the cytosolic [Ca^{2+}] in erythrocytes from Ptpre$^{-/-}$ and control mice; then we characterized the activity of the Gardos channel. The basal cytosolic [Ca^{2+}] was slightly, but not significantly, higher in Ptpre$^{-/-}$ red cells than in controls (Fig. 2c). The increase in intracellular [Ca^{2+}]$_i$ produced by addition of a small amount of the ionophore ionomycin (50 nM) to a cellular suspension containing [Ca^{2+}] in the physiological range (0.5 mM) (Fig. 2c), or of a relatively high concentration of ionomycin (1 μM) to a low Ca^{2+}-containing medium (7 μM) (Fig. 2d), was significantly higher in erythrocytes from Ptpre$^{-/-}$ than in control red cells. In addition, [Ca^{2+}]$_i$ accumulation induced by sodium vanadate, an inhibitor of plasma membrane Ca^{2+} pump [7], was higher in Ptpre$^{-/-}$ red cells than in controls (Fig. 2c; $P<0.05$). We carried out experiments at relative long incubation time (20 min) with and without vanadate. The [Ca^{2+}]$_i$ markedly increased in Ptpre$^{-/-}$ erythrocytes treated with vanadate compared to controls, whereas no major differences were evident between untreated red cells (Fig. 2c). The higher [Ca^{2+}]$_i$ levels observed in Ptpre$^{-/-}$erythrocytes after inhibition of the Ca^{2+} pumping by vanadate suggest the existence of a vanadate independent component contributing to [Ca^{2+}]$_I$, which may be represented by the non-selective voltage dependent cation channel (NSVDC channel). [46]

Erythrocytes from Ptpre$^{-/-}$ mice exhibited higher the Ca^{2+} activated-K^+ (Gardos) channel activity than those from wild-type mice, suggesting that a functionally up-regulated Gardos channel may participate to generation of dense red cells in Ptpre$^{-/-}$mice (Fig. 3a). In order to assess the effects of the absence of PTPε on the kinetic properties of the Ca^{2+} activated-K^+ channel, the K^+ influx was measured at varying concentrations of extracellular Ca^{2+} in the presence of the calcium ionophore A21387 with and without charybdotoxin (ChTX), a known inhibitor of the Gardos channel. The ChTX-sensitive K^+ influx kinetic analysis showed higher V_{max} (wild-type: 5.84±0.1 *vs* Ptpre$^{-/-}$: 9.17±0.2 mM cell/ min; $P<0.05$, $n=5$) and lower affinity for Ca^{2+} (K_m 0.33±0.01 *vs* 0.24±0.02 μM, $P<0.05$, $n=5$) in red cell lacking PTPε compared to wild-type erythrocytes.

In order to evaluate the effects of *in vivo* Gardos channel inhibition, Ptpre$^{-/-}$ mice were treated with clotrimazole (CLT), a known inhibitor of the Gardos channel activity [22,29]. Oral administration of CLT determined a reduction in red cell dehydration in Ptpre$^{-/-}$ mice, while no significant differences were observed in wild-type mice (Fig. 3b). With CLT treatment D_{20} and CHCM values decreased in Ptpre$^{-/-}$mice from 1,096 ±0,002 to 1,092 ± 0,001 ($n=6$; $P<0.05$) and from 29.9 ± 0.2 g/dL ($n=6$) to 27.8 ± 0.2 g/dL ($n=6$; $P<0.05$), respectively; D_{20} and CHCM values were unchanged in wild-type mice treated with CLT, as

previously reported in other mouse strains [22]. Red cell K^+ content significantly rose in Ptpre$^{-/-}$mice from 378.4 ± 11 mmol/Kg Hb (n=6) to 412.5 ± 10 mmol/Kg Hb (n=6; P<0.05) with CLT treatment.

These data demonstrate that the abnormally higher density of Ptpre$^{-/-}$mouse erythrocytes is the consequence of a constitutive activation of the Gardos channel induced either directly or indirectly by the absence of PTPε.

Functional relationship between Ca^{2+} activated-K^+ channel, PTPε and Fyn in red cells

Previous studies in human red cells have suggested that the activity of the Ca^{2+} activated-K^+ (Gardos) channel might be regulated by phosphorylation-dephosphorylation events, involving kinases, such protein kinase C, and phosphatases whose identity is still unknown [34]. We therefore evaluated the effects of the PKC inhibitor, calphostin C[34], and of the SFKs inhibitor, PP1 [5,35], on Gardos channel activity in wild-type and PTPε knockout mouse red cells. As shown in Fig. 3c, calphostin C and PP1 inhibited the Gardos channel activity in both mouse strains, indicating that both PKC and Src-family-tyrosine kinases may be involved in regulating the Gardos channel. It is interesting to note that in PTPε knockout mouse red cells, Calphostin C only partially reduced the Gardos channel activity, whereas inhibition by PP1 reached values similar to those observed in untreated wild-type mouse erythrocytes, suggesting a more complex regulating pathway comprising both calphostin-C dependent and independent components.

Studies in other cell types have proposed a functional cross-talk between SFKs, in particular Fyn, and Ca^{2+} channels [47,48]. Thus, we studied the expression and the activity of two SFKs: Fyn, Hck and Yes. The expression of Fyn, Hck and Yes was similar in red cells from both mouse strains (data not shown). In contrast, Fyn and Yes kinase activity was significantly higher in mouse red cells lacking PTPε than in controls (Fig. 3d, e), while Hck kinase activity was similar in both mouse strains, suggesting a action of PTPε on Fyn and Yes kinases, which show high structural homology and overlapping functions [49]. These data indicate a role of PTPε as an integral component of signal transduction pathways in mouse red cells. To verify this hypothesis, we used a proteomic approach to study and characterize the tyrosine phosphorylation profile of red cell membrane proteins in mice lacking PTPε.

PTPε absence affects the red cell membrane tyrosine phosphoproteome and modifies cell signaling network topology

To analyse the tyrosine phosphorylation pattern of red cell membrane proteins we first evaluated the anti-phosphotyrosine immunoblotting profile of red cell membrane protein from wild-type and PTPε knockout mice (Fig. 4). Red cells lacking PTPε exhibited stronger tyrosine (Tyr) phosphorylation of various membrane proteins compared to wild-type erythrocytes, supporting an important role of PTPε in mouse erythrocytes signaling pathways. In order to identify the erythrocyte membrane proteins, which differ in Tyr-phosphorylation, we analyzed both (i) anti-phosphotyrosine immunoprecipitated proteins, separated by mono-dimensional electrophoresis; and (ii) erythrocyte membrane proteins separated by two-dimensional gel electrophoresis (2D). 2Ds were performed in duplicated gels: one was blotted and probed with anti-phosphotyrosine antibodies, while the other one was used for protein identification (n=20; Fig. 4a, b). The relative quantification of immunoreactivity revealed increased amounts of Tyr-phosphorylated proteins in mice lacking PTPε compared to wild-type mice as well as the presence of proteins that were Tyr-phosphorylated only in either knockout or wild-type mouse red cells. Bands (1D) and spots (2D) differently Tyr-phosphorylated in Ptpre$^{-/-}$ mice *vs* wild-type were localized in the corresponding Coomassie-stained gel from the Western-blots by image analysis, excised and

subjected to peptide mass fingerprinting by MALDI-TOF (Fig. 4, Table 2). Three major clustered groups of proteins with differences in Tyr-phosphorylation were identified: membrane skeletal proteins, chaperones and proteosomes (Fig. 4c, Table 2). In addition, we identified the Tyr- phosphorylated residues in tropomyosin- 3 from wild-type red cells and respectively in α-spectrin and ankyrin from red cells lacking PTPε (Fig. 5, Table 3), raising important questions about the influence of protein Tyr-phosphorylation on the overall organization of signaling networks in mouse red blood cells. The sites of phosphorylation have been confirmed by demonstration of mass shift of the peptides following phosphatase treatment (see supplementary data).

To investigate the influence of modulation of protein Tyr-phosphorylation on the regulation of red cell signaling mechanisms we performed a signaling network computational analysis [50–52]. Such analysis can be useful to better direct further experiments and highlight new potential regulatory mechanisms. We first identified signaling sub-networks specifically correlated to the activity of the identified Tyr-phosphorylated proteins. To reduce complexity, but still achieve high significance, we initially limited our analysis to the first interacting-neighbor. As shown in Fig. 6, the 11 phosphorylated proteins identified in wild-type erythrocytes sustain a network comprising 241 proteins and 724 binary interactions. In contrast, the 16 phosphorylated proteins identified in Ptpre$^{-/-}$ red cells sustain a network comprising 294 proteins and 838 binary interactions (Fig. 6). Analysis of the large-scale structure of the two sub-networks showed that both networks display a scale-free topology [53,54], a topology characteristic of information processing structures. It is of interest that the comparison of wild-type *vs* Ptpre$^{-/-}$ Tyr-phosphorylated protein sub-networks reveals that both wild-type and Ptpre$^{-/-}$ phosphorylated sub-networks display equivalent capability to generate functional protein clusters (almost identical average clustering coefficient, not shown). Based on this observation, we proceeded with a modular decomposition of the networks [55]. We applied the MCODE algorithm, which has been shown to be able to identify topological clusters corresponding to functional protein complexes in signaling networks [41]. Fig. 7 shows the clusters identified by analysis. Seven distinct clusters in wild-type and six clusters in Ptpre$^{-/-}$ networks were identified. Clusters 2, 3 and 5 were identical in wild-type *versus* Ptpre$^{-/-}$ networks, making unlikely that proteins constitutive of these clusters are responsible for the morphological differences between wild-type and Ptpre$^{-/-}$ red blood cells (Fig. 7). Thus, these clusters were not further analyzed. In contrast, clusters 1, 4, 6 and 7 were either quantitatively and/or qualitatively different. Cluster 1 (*Fyn cluster*) was qualitatively identical in wild-type *versus* Ptpre$^{-/-}$ cells, being formed by the same proteins and interactions, but was quantitatively different: the main cluster regulatory protein Fyn (alone accounting for about 30% of total cluster interactions) was significantly more phosphorylated in Ptpre$^{-/-}$ cells (+ 375%, Fig. 6 and 7). In contrast, cluster 4 was qualitatively different. Here, beta-actin was equally Tyr-phosphorylated but tropomyosin-3, F-actin and calponin-1 were absent in the Ptpre$^{-/-}$ cell cluster. Cluster 6 and 7 were also qualitatively different. Indeed, the Ptpre$^{-/-}$ cluster 6 counted only proteasome subunits, with the subunit beta type 4 Tyr-phosphorylated. Finally, cluster 7 was present only in wild-type red cells, with alpha-spectrin highly Tyr-phosphorylated with beta-spectrin and adducin involved (Fig. 7a).

Based on data from the computational analysis we further analysed cluster 1 (*Fyn cluster*), which presented the highest score (2.00) and subsequently the highest probability to occur *in vivo* (Fig. 7a). In cluster 1, we considered Syk expression and Syk kinase activity in both red cell ghost and cytosol fractions from both mouse strains. Syk protein was similarly expressed in both mouse strains, and it was more abundant in cytosol fraction than in ghost fraction (data not shown). Although Syk protein expression was similar in wild-type and Ptpre$^{-/-}$ mice, Syk activity in red cell ghost and cytosol fractions was higher in wild-type than in Ptpre$^{-/-}$ mice (Fig. 7b). To determine whether the differences in the activity of Syk

kinase from wild-type and Ptpre$^{-/-}$ mouse red cells were functionally relevant, we evaluated the ability of Syk to Tyr-phosphorylate two known endogenous substrates: band 3 and synuclein, which have been described to be Syk targets [35,38]. As shown in Fig 7c, Tyr-phosphorylation of band 3 and synuclein by Syk kinase was higher in presence of Syk immunopurified from wild-type mouse red cells than with that from mice lacking PTPε, suggesting a novel signaling pathway, which involved Fyn and Syk participating to regulation of red cell morphology (Fig. 7).

4. DISCUSSION

Changes in proteins Tyrosine-phosphorylation state and modulation of membrane channels are part of the cell signaling transduction pathways and play a crucial role in cell homeostasis. In red cells the absence of PTPε markedly affects signaling transduction pathways as supported by (i) the abnormal regulation of the Ca^{2+} activated-K^+ channel; (ii) the perturbation of red cell membrane Tyr-phosphoproteome and (iii) the changes in cell signaling network topology.

The Ca^{2+} activated-K^+ channel is important in maintaining red cell volume/surface ratio and is abnormally activated in some diseased red cells [22,29,56]. Although data on human red cells suggested that the activity of the Ca^{2+} activated-K^+ channel might be modulated by phosphorylation-dephosphorylation events, its regulating pathway is still under investigation [34]. Studies in various cell types indicate that the regulation of the Ca^{2+} activated-K^+ channel might involve not only protein kinase-C (PKC) and protein kinase A (PKA), but also calmodulin and MAP-kinase pathway [57–59], suggesting a complex signaling network. In addition, SFKs have been recently described to modulate different types of Ca^{2+} channel and to functionally cross-talk with PKC [60]. In mouse red cells, the ability of the SFKs inhibitor PP1 to reduce Gardos channel activity suggests that SFKs might be part of the signaling pathway regulating the Gardos channel. Fyn, Yes and Hck are members of the SFKs [60]. In red cells lacking PTPε, the activity of Fyn and Yes were increased, while Hck activity was similar in both mouse strains, suggesting a cross-talk between Fyn/ Yes, which show high structural homology, and PTP-ε towards the Gardos channel either directly or indirectly downstream of PKC, favoring an unbalance between the kinase(s) and phosphatase(s) involved in Gardos channel regulating pathway.

Since Fyn is part of signal transduction pathways in other cell types [61–63], we then evaluated whether PTPε might contribute to more complex modification of red cell membrane phosphoproteome. We studied the red cell membrane tyrosine phosphorylation profile in both mouse strains and observed that the absence of PTP-ε markedly affects the tyrosine phosphorylation state of three major clustered groups of proteins (i) the membrane skeletal proteins (ii) the chaperones and (iii) the proteosomes together with the Src-family kinase Fyn, raising important questions about the influence of protein Tyr-phosphorylation on the overall organization of the signaling networks in mouse red cells. In order to further analyze the proteomic data, we performed a signaling network computational analysis. Although a mathematical abstraction should not be considered an experimental proof, as it always needs an empirical validation, this analysis suggests some interesting observations. The cluster 1, the *Fyn cluster*, seems a good candidate to be validated as a restricted set of interacting proteins participating to regulation of red cell morphology of Ptpre$^{-/-}$ mice. The most interesting proteins are PLC-gamma1, PI3K-alpha, Ezrin, Syk and Sit. All, but Ezrin, are directly interacting with Fyn and are potentially involved in membrane regulation (according to Gene Ontology analysis, see methods). Indeed, PI3K-alpha, Ezrin, Syk and PLC-gamma1 are up-stream regulators or downstream effectors of rho small GTPases, whose role in membrane assembly is well known in different cell types and recently shown also in mouse red cells [64,65]. Notably, these proteins are substrates of Fyn

phosphorylation and thus are likely regulated by Fyn itself. Between them in cluster 1, we experimentally tested Syk kinase activity in red cells from both mouse strains. Syk kinase activity was indeed up-regulated in wild-type red cells compared to Ptpre$^{-/-}$ mouse erythrocytes (Fig. 7). The modulation of Syk kinase activity validates the network computational analysis and supports new functional interactions between Syk and Fyn, which activity may be in turn modulated by PTPε (Fig. 7b).

Cluster 7 is present in wild-type erythrocytes and absent in Ptpre$^{-/-}$ red cells. This is of interest because adducin regulates assembly of spectrins, which are the predominant components of red cell membrane skeleton, essential in determining the properties of the membrane including its shape and deformability. Although there is evidence of adducin serine-threonine phosphorylation in red cells, no data are available on adducin Tyr-phosphorylation, except for *in vitro* studies of adducin regulation [65,66]. Recently, it was shown that β-adducin can be Tyr-phosphorylated in the C-terminal tail domain by Fyn in COS-7 cells and in central nervous system cells [67]. In mouse red cells, adducin is highly Tyr-phosphorylated in Ptpre$^{-/-}$ mice compared to wild-type mice, suggesting an interaction between Fyn and adducin, which may modify the adducin ability to actin-interact form with spectrins, supporting the absence of cluster 7 in Ptpre$^{-/-}$ red cells.

Overall, the network topological analysis may suggest that absence of PTPε in red cells leads to Fyn hyper-phosphorylation, and may trigger the formation of an active protein complex able to affect cytoskeleton dynamics and red cell morphology in Ptpre$^{-/-}$ mice. Exclusion of negative regulators (calponin-1, tropomyosin-3) and of structural components (adducin, α- β-spectrins) is in keeping with the hypothesis of an unbalanced cytoskeleton in Ptpre$^{-/-}$ red cells, dependent on the dynamics of Fyn-activated proteins. Further studies are required to experimentally test this hypothesis, by evaluating the activation state of other proteins belonging to the *Fyn cluster* and the effects of their inhibition, alone or in combination, on red cell features.

Supplementary Material

Refer to Web version on PubMed Central for supplementary material.

Abbreviations

RBC red blood cells

Acknowledgments

Preliminary data have been presented at the American Society of Hematology (ASH) meeting, San Diego, CA 2003. Supported by NIH grants DK50422 (cb, ldf), FIRB-grant RBNE01XHME (ldf, ft, ai) and PRIN (ldf, ai).

REFERENCES

1. Tanuma N, Shima H, Shimada S, Kikuchi K. Reduced tumorigenicity of murine leukemia cells expressing protein-tyrosine phosphatase, PTPepsilon C. Oncogene. 2003; 22:1758–1762. [PubMed: 12660811]
2. Tanuma N, Shima H, Nakamura K, Kikuchi K. Protein tyrosine phosphatase epsilonC selectively inhibits interleukin-6- and interleukin- 10-induced JAK-STAT signaling. Blood. 2001; 98:3030–3034. [PubMed: 11698287]
3. Tanuma N, Nakamura K, Shima H, Kikuchi K. Protein-tyrosine phosphatase PTPepsilon C inhibits Jak-STAT signaling and differentiation induced by interleukin-6 and leukemia inhibitory factor in M1 leukemia cells. J Biol Chem. 2000; 275:28216–28221. [PubMed: 10859312]

4. Minetti G, Ciana A, Balduini C. Differential sorting of tyrosine kinases and phosphotyrosine phosphatases acting on band 3 during vesiculation of human erythrocytes. Biochem J. 2004; 377:489–497. [PubMed: 14527338]
5. Zipser Y, Piade A, Barbul A, Korenstein R, Kosower NS. Ca2+ promotes erythrocyte band 3 tyrosine phosphorylation via dissociation of phosphotyrosine phosphatase from band 3. Biochem J. 2002; 368:137–144. [PubMed: 12175337]
6. Huyer G, Liu S, Kelly J, Moffat J, et al. Mechanism of inhibition of protein-tyrosine phosphatases by vanadate and pervanadate. J Biol Chem. 1997; 272:843–851. [PubMed: 8995372]
7. Tiffert T, Lew VL. Kinetics of inhibition of the plasma membrane calcium pump by vanadate in intact human red cells. Cell Calcium. 2001; 30:337–342. [PubMed: 11733940]
8. Romero PJ, Romero EA. New vanadate-induced Ca2+ pathway in human red cells. Cell Biol Int. 2003; 27:903–912. [PubMed: 14585284]
9. Kaiserova K, Lakatos B, Peterajova E, Orlicky J, Varecka L. Investigation of properties of the Ca2+ influx and of the Ca2+-activated K+ efflux (Gardos effect) in vanadate-treated and ATP-depleted human red blood cells. Gen Physiol Biophys. 2002; 21:429–442. [PubMed: 12693714]
10. Bordin L, Brunati AM, Donella-Deana A, Baggio B, et al. Band 3 is an anchor protein and a target for SHP-2 tyrosine phosphatase in human erythrocytes. Blood. 2002; 100:276–282. [PubMed: 12070037]
11. Zipser Y, Kosower NS. Phosphotyrosine phosphatase associated with band 3 protein in the human erythrocyte membrane. Biochem J. 1996; 314(Pt 3):881–887. [PubMed: 8615784]
12. Siemon H, Schneider H, Fuhrmann GF. Vanadium increases selective K+-permeability in human erythrocytes. Toxicology. 1981; 22:271–278. [PubMed: 7342369]
13. Peretz A, Gil-Henn H, Sobko A, Shinder V, et al. Hypomyelination and increased activity of voltage-gated K(+) channels in mice lacking protein tyrosine phosphatase epsilon. Embo J. 2000; 19:4036–4045. [PubMed: 10921884]
14. Sully V, Pownall S, Vincan E, Bassal S, et al. Functional abnormalities in protein tyrosine phosphatase epsilon-deficient macrophages. Biochem Biophys Res Commun. 2001; 286:184–188. [PubMed: 11485326]
15. Chiusaroli R, Knobler H, Luxenburg C, Sanjay A, et al. Tyrosine phosphatase epsilon is a positive regulator of osteoclast function in vitro and in vivo. Mol Biol Cell. 2004; 15:234–244. [PubMed: 14528021]
16. Gil-Henn H, Elson A. Tyrosine phosphatase-epsilon activates Src and supports the transformed phenotype of Neu-induced mammary tumor cells. J Biol Chem. 2003; 278:15579–15586. [PubMed: 12598528]
17. Elson A, Leder P. Protein-tyrosine phosphatase epsilon. An isoform specifically expressed in mouse mammary tumors initiated by v-Ha-ras OR neu. J Biol Chem. 1995; 270:26116–26122. [PubMed: 7592814]
18. Elson A, Leder P. Identification of a cytoplasmic, phorbol ester-inducible isoform of protein tyrosine phosphatase epsilon. Proc Natl Acad Sci U S A. 1995; 92:12235–12239. [PubMed: 8618876]
19. Toledano-Katchalski H, Tiran Z, Sines T, Shani G, et al. Dimerization in vivo and inhibition of the nonreceptor form of protein tyrosine phosphatase epsilon. Mol Cell Biol. 2003; 23:5460–5471. [PubMed: 12861030]
20. Bennekou P, de Franceschi L, Pedersen O, Lian L, et al. Treatment with NS3623, a novel Cl-conductance blocker, ameliorates erythrocyte dehydration in transgenic SAD mice: a possible new therapeutic approach for sickle cell disease. Blood. 2001; 97:1451–1457. [PubMed: 11222393]
21. Brugnara C, de Franceschi L, Alper SL. Inhibition of Ca(2+)-dependent K+ transport and cell dehydration in sickle erythrocytes by clotrimazole and other imidazole derivatives. J Clin Invest. 1993; 92:520–526. [PubMed: 8326017]
22. De Franceschi L, Rivera A, Fleming MD, Honczarenko M, et al. Evidence for a protective role of the Gardos channel against hemolysis in murine spherocytosis. Blood. 2005; 106:1454–1459. [PubMed: 15855279]

23. De Franceschi L, Fumagalli L, Olivieri O, Corrocher R, et al. Deficiency of Src family kinases Fgr and Hck results in activation of erythrocyte K/Cl cotransport. J Clin Invest. 1997; 99:220–227. [PubMed: 9005990]
24. De Franceschi L, Beuzard Y, Brugnara C. Sulfhydryl oxidation and activation of red cell K(+)-Cl- cotransport in the transgenic SAD mouse. Am J Physiol. 1995; 269:C899–C906. [PubMed: 7485459]
25. Perrotta S, Miraglia del Giudice E, Alloisio N, Sciarratta G, et al. Mild elliptocytosis associated with the alpha 34 Arg-->Trp mutation in spectrin Genova (alpha I/74). Blood. 1994; 83:3346–3349. [PubMed: 8193371]
26. Miraglia del Giudice E, Iolascon A, Pinto L, Nobili B, Perrotta S. Erythrocyte membrane protein alterations underlying clinical heterogeneity in hereditary spherocytosis. Br J Haematol. 1994; 88:52–55. [PubMed: 7803256]
27. Fairbanks G, Steck TL, Wallach DF. Electrophoretic analysis of the major polypeptides of the human erythrocyte membrane. Biochemistry. 1971; 10:2606–2617. [PubMed: 4326772]
28. de Franceschi L, Turrini F, Honczarenko M, Ayi K, et al. In vivo reduction of erythrocyte oxidant stress in a murine model of beta-thalassemia. Haematologica. 2004; 89:1287–1298. [PubMed: 15531450]
29. De Franceschi L, Saadane N, Trudel M, Alper SL, et al. Treatment with oral clotrimazole blocks Ca(2+)-activated K+ transport and reverses erythrocyte dehydration in transgenic SAD mice. A model for therapy of sickle cell disease. J Clin Invest. 1994; 93:1670–1676. [PubMed: 7512989]
30. Lindner A, Hinds TR, Davidson RC, Vincenzi FF. Increased cytosolic free calcium in red blood cells is associated with essential hypertension in humans. Am J Hypertens. 1993; 6:771–779. [PubMed: 8110431]
31. Kaestner L, Tabellion W, Weiss E, Bernhardt I, Lipp P. Calcium imaging of individual erythrocytes: problems and approaches. Cell Calcium. 2006; 39:13–19. [PubMed: 16242187]
32. Bauer PJ. Affinity and stoichiometry of calcium binding by arsenazo III. Anal Biochem. 1981; 110:61–72. [PubMed: 7212270]
33. Rivera A, Rotter MA, Brugnara C. Endothelins activate Ca(2+)-gated K(+) channels via endothelin B receptors in CD-1 mouse erythrocytes. Am J Physiol. 1999; 277:C746–C754. [PubMed: 10516105]
34. Rivera A, Jarolim P, Brugnara C. Modulation of Gardos channel activity by cytokines in sickle erythrocytes. Blood. 2002; 99:357–603. [PubMed: 11756192]
35. Brunati AM, Bordin L, Clari G, James P, et al. Sequential phosphorylation of protein band 3 by Syk and Lyn tyrosine kinases in intact human erythrocytes: identification of primary and secondary phosphorylation sites. Blood. 2000; 96:1550–1557. [PubMed: 10942405]
36. Stocker JW, De Franceschi L, McNaughton-Smith GA, Corrocher R, et al. ICA-17043, a novel Gardos channel blocker, prevents sickled red blood cell dehydration in vitro and in vivo in SAD mice. Blood. 2003; 101:2412–2418. [PubMed: 12433690]
37. Narisawa-Saito M, Silva AJ, Yamaguchi T, Hayashi T, et al. Growth factor-mediated Fyn signaling regulates alpha-amino-3- hydroxy-5-methyl-4-isoxazolepropionic acid (AMPA) receptor expression in rodent neocortical neurons. Proc Natl Acad Sci U S A. 1999; 96:2461–2466. [PubMed: 10051665]
38. Negro A, Brunati AM, Donella-Deana A, Massimino ML, Pinna LA. Multiple phosphorylation of alpha-synuclein by protein tyrosine kinase Syk prevents eosin-induced aggregation. Faseb J. 2002; 16:210–212. [PubMed: 11744621]
39. Torres MP, Thapar R, Marzluff WF, Borchers CH. Phosphatase-directed phosphorylation-site determination: a synthesis of methods for the detection and identification of phosphopeptides. J Proteome Res. 2005; 4:1628–1635. [PubMed: 16212415]
40. Shannon P, Markiel A, Ozier O, Baliga NS, et al. Cytoscape: a software environment for integrated models of biomolecular interaction networks. Genome Res. 2003; 13:2498–2504. [PubMed: 14597658]
41. Bader GD, Hogue CW. An automated method for finding molecular complexes in large protein interaction networks. BMC Bioinformatics. 2003; 4:2. [PubMed: 12525261]

42. Hu Z, Mellor J, Wu J, Yamada T, et al. VisANT: data-integrating visual framework for biological networks and modules. Nucleic Acids Res. 2005; 33:W352–W357. [PubMed: 15980487]
43. Maere S, Heymans K, Kuiper M. BiNGO: a Cytoscape plugin to assess overrepresentation of gene ontology categories in biological networks. Bioinformatics. 2005; 21:3448–3449. [PubMed: 15972284]
44. de Jong K, Larkin SK, Styles LA, Bookchin RM, Kuypers FA. Characterization of the phosphatidylserine-exposing subpopulation of sickle cells. Blood. 2001; 98:860–867. [PubMed: 11468189]
45. Koopman G, Reutelingsperger CP, Kuijten GA, Keehnen RM, et al. Annexin V for flow cytometric detection of phosphatidylserine expression on B cells undergoing apoptosis. Blood. 1994; 84:1415–1420. [PubMed: 8068938]
46. Bennekou P, Kristensen BI, Christophersen P. The human red cell voltage-regulated cation channel. The interplay with the chloride conductance, the Ca(2+)-activated K(+) channel and the Ca(2+) pump. J Membr Biol. 2003; 195:1–8. [PubMed: 14502420]
47. Nitabach MN, Llamas DA, Araneda RC, Intile JL, et al. A mechanism for combinatorial regulation of electrical activity: Potassium channel subunits capable of functioning as Src homology 3-dependent adaptors. Proc Natl Acad Sci U S A. 2001; 98:705–710. [PubMed: 11149959]
48. Ling S, Woronuk G, Sy L, Lev S, Braun AP. Enhanced activity of a large conductance, calcium-sensitive K+ channel in the presence of Src tyrosine kinase. J Biol Chem. 2000; 275:30683–30689. [PubMed: 10893418]
49. Sandilands E, Brunton VG, Frame MC. The membrane targeting and spatial activation of Src, Yes and Fyn is influenced by palmitoylation and distinct RhoB/RhoD endosome requirements. J Cell Sci. 2007; 120:2555–2564. [PubMed: 17623777]
50. Bhalla US, Iyengar R. Emergent properties of networks of biological signaling pathways. Science. 1999; 283:381–387. [PubMed: 9888852]
51. Strogatz SH. Exploring complex networks. Nature. 2001; 410:268–276. [PubMed: 11258382]
52. Jordan JD, Landau EM, Iyengar R. Signaling networks: the origins of cellular multitasking. Cell. 2000; 103:193–200. [PubMed: 11057893]
53. Barabasi AL, Oltvai ZN. Network biology: understanding the cell's functional organization. Nat Rev Genet. 2004; 5:101–113. [PubMed: 14735121]
54. Jeong H, Tombor B, Albert R, Oltvai ZN, Barabasi AL. The large-scale organization of metabolic networks. Nature. 2000; 407:651–654. [PubMed: 11034217]
55. Hartwell LH, Hopfield JJ, Leibler S, Murray AW. From molecular to modular cell biology. Nature. 1999; 402:C47–C52. [PubMed: 10591225]
56. Brugnara C, De Franceschi L, Bennekou P, Alper SL, Christophersen P. Novel therapies for prevention of erythrocyte dehydration in sickle cell anemia. Drug News Perspect. 2001; 14:208–220. [PubMed: 12819792]
57. Sazonova OV, Blishchenko EY, Tolmazova AG, Khachin DP, et al. Stimulation of fibroblast proliferation by neokyotorphin requires Ca influx and activation of PKA, CaMK II and MAPK/ERK. Febs J. 2007; 274:474–484. [PubMed: 17229152]
58. Struthers RS, Xie Q, Sullivan SK, Reinhart GJ, et al. Pharmacological characterization of a novel nonpeptide antagonist of the human gonadotropin-releasing hormone receptor, NBI-42902. Endocrinology. 2007; 148:857–867. [PubMed: 17095587]
59. Si H, Grgic I, Heyken WT, Maier T, et al. Mitogenic modulation of Ca2+ -activated K+ channels in proliferating A7r5 vascular smooth muscle cells. Br J Pharmacol. 2006; 148:909–917. [PubMed: 16770324]
60. Cohen DM. SRC family kinases in cell volume regulation. Am J Physiol Cell Physiol. 2005; 288:C483–C493. [PubMed: 15692147]
61. Toledano-Katchalski H, Kraut J, Sines T, Granot-Attas S, et al. Protein tyrosine phosphatase epsilon inhibits signaling by mitogen-activated protein kinases. Mol Cancer Res. 2003; 1:541–550. [PubMed: 12754301]
62. Toledano-Katchalski H, Elson A. The transmembranal and cytoplasmic forms of protein tyrosine phosphatase epsilon physically associate with the adaptor molecule Grb2. Oncogene. 1999; 18:5024–5031. [PubMed: 10490839]

63. Tiran Z, Peretz A, Attali B, Elson A. Phosphorylation-dependent regulation of Kv2.1 Channel activity at tyrosine 124 by Src and by protein-tyrosine phosphatase epsilon. J Biol Chem. 2003; 278:17509–17514. [PubMed: 12615930]

64. Bishop AL, Hall A. Rho GTPases and their effector proteins. Biochem J. 2000; 348(Pt 2):241–255. [PubMed: 10816416]

65. Kalfa TA, Pushkaran S, Mohandas N, Hartwig JH, et al. Rac GTPases regulate the morphology and deformability of the erythrocyte cytoskeleton. Blood. 2006

66. Matsuoka Y, Hughes CA, Bennett V. Adducin regulation. Definition of the calmodulin-binding domain and sites of phosphorylation by protein kinases A and C. J Biol Chem. 1996; 271:25157–25166. [PubMed: 8810272]

67. Gotoh H, Okumura N, Yagi T, Okumura A, et al. Fyn-induced phosphorylation of beta-adducin at tyrosine 489 and its role in their subcellular localization. Biochem Biophys Res Commun. 2006; 346:600–605. [PubMed: 16765915]

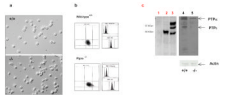

Fig. 1. The absence of PTPε causes abnormal red cell morphology and generation of dense erythrocytes

(a) red cell morphology; **(b)** red cell histograms generated for erythrocyte volume (RBC V) and cell hemoglobin concentration (RBC HC) and plot of RBC HC (*x-axis*) *vs* RBC volume (*y-axis*) from wild-type (+/+) and Ptpre$^{-/-}$(−/−) mice are presented; **(c)** Immunoblot analysis of PTPε protein expression in extracts of HEK293 cells transiently expressing PTPε protein and in red cell membrane from wild-type and Ptpre$^{-/-}$ mice [17,18]. Lane 1: HEK293 cells transfected with empty vector; lane 2: HEK293 cells transfected with vector expressing cytoplasmatic PTPε protein; lane 3: HEK293 cells transfected with vector expression both cytoplasmatic and receptor PTPε protein; lane 4: wild-type (+/+) mouse red cells and lane 5: Ptpre$^{-/-}$(−/−) mouse red cells. Expression of actin was used for loading control for mouse red cells. One out of 6 independent experiments with similar results are presented.

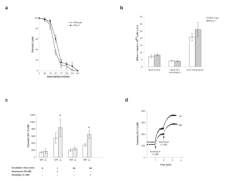

Fig. 2. Red cells lacking PTPε show higher susceptibility to osmotic stress and changes in cell Ca^{2+} content

(a) Red cell osmotic fragility curves for wild-type (+/+, open circle) and Ptpre$^{-/-}$(−/−, solid circle) mouse red cells. Data are presented as means ± SD (*n*=10); **(b)** Activities of Na/K pump, Na/K/2Cl cotransport and K/Cl cotransport (KCC) in red cells from wild-type (white bar) and in Ptpre$^{-/-}$(gray bar) mice. Data are presented as means ± SD (*n*=12); **(c)** Cytosolic $[Ca^{2+}]_c$ in red blood cells from wild-type (+/+, white bar) and in Ptpre$^{-/-}$(−/−, light gray bar) mice before and after exposure to ionomycin or to sodium vanadate. The increase in $[Ca^{2+}]_c$ was measured, in cellular suspensions containing 0.5 mM $[Ca^{2+}]$,1 min after addition of 50 nM ionomycin (*n*=12), or 20 min after 1 mM vanadate addition (*n*=6). Data are reported means±SD; $P < 0.05$ for ionomycin and $P < 0.01$ for vanadate, compared to wild-type; **(d)** $[Ca^{2+}]_c$ obtained by addition of 1 μM ionomycin to cellular suspensions containing Ca^{2+} (7 μM) in wild-type (+/+) and in Ptpre$^{-/-}$(−/−) mice (*n*=6); * $P<0.05$ compared to wild-type.

Fig. 3. In Ptpre$^{-/-}$ mouse red cells the Ca^{2+} activated-K^+ channel activity is abnormally activated and is modulated by Src-family kinase

(a) The Ca^{2+} activated-K^+ channel (Gardos channel) activity in red cells from wild-type (+/+) and in PTPε knockout (Ptpre$^{-/-}$;−/−) mice. **P*<0.05 compared to wild-type (*n*=6); **(b)** Effects of clotrimazole treatment (CLT: 160 mg/Kg twice administred orally twice a day) on red cells density profiles in wild-type and PTPε knockout (Ptpre$^{-/-}$) mice. Phthalate density profiles are presented at baseline and after 12 days of CLT treatment. Data are presented as means ± SD (*n*=6); **(c)** Effects of calphostin C (1 μM), PKC inhibitor, and PP1 (10 μM), SFKs inhibitor, on the Gardos channel activity in red cells from wild-type (+/+) and in Ptpre$^{-/-}$(−/−) mice. Data are presented as means ± SD (*n*=6); **P*<0.05 compared to untreated red cells; **(d)** Fyn and Hck kinase activity in red cells from wild-type (+/+) and in Ptpre$^{-/-}$(−/−) mice. The immunoprecipitates were subjected to *in vitro* kinase assays (*KA*) and then to western-blot analysis (WB) with the corresponding specific antibody (*WB*). Shown is a representative experiments of 6 performed with similar results. **(e)** Fyn kinase assays (*KA*) was also determined by measuring phosphorylation levels of enolase, as exogenous substrate. *Lane 1*: beads, *lane 2*: beads with anti-Fyn; *lane 3*: anti-Fyn immunoprecipitated from red cells of wild-type (+/+) mice; *lane 4:* anti-Fyn immunoprecipitated from red cells of Ptpre$^{-/-}$(−/−) mice. Molecular weight markers are shown and the mobility of enolase is indicated. A representative experiments of 3 performed with similar results is presented.

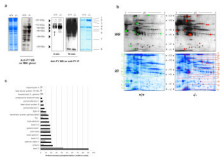

Fig. 4. The absence of PTPε modifies the red cells membrane Tyrosine-phosphoproteome

Western-blot analysis with specific anti-phosphotyrosine antibodies of red cell ghosts from wild-type (+/+) and in Ptpre$^{-/-}$(−/−) mice. **(a)** Red cell ghosts were separated by mono-dimensional electrophoresis and blotted with specific anti-phosphotyrosine (anti-PY WB) or underwent immunoprecipitation with specific anti-phosphotyrosine antibodies (anti-PY WB on anti-PY IP; two different time exposure are shown: 5 and 10 min) and then either used for Western-blot analysis with specific anti-phosphotyrosine antibodies or stained with colloidal Coomassie for protein identification **(b)** Red cell ghosts were separated by two-dimensional electrophoresis (2D; *n*=20). Twin gels were run, one was used for Western-blot analysis with specific anti-phosphotyrosine antibodies, the other one was stained with colloidal Coomassie for protein identification. Red and green spots indicated the differently tyrosine phosphorylated proteins respectively in wild-type (+/+) and in Ptpre$^{-/-}$(−/−) mice. **(d)** Relative quantification of immunoreactivity of tyrosine-phosphorylated proteins in red cells from wild-type (+/+, gray bar) and Ptpre$^{-/-}$(−/−; black bar) mice. Data are presented as median (*n*=6).

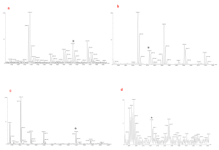

Fig. 5. Phosphorylated peptides from red cell membrane of wild-type mice (a) tropomyosine-3 and from Ptpre$^{-/-}$mice (b–c) spectrin alfa and (d) ankyrin

Red cell membrane were separated by two-dimensional electrophoresis (2D) Phosphorylated peptides were analyzed by MALDI-MS in reflectron mode using a-cyano-4-hydroxycinnamic acid as the matrix. Asterisk indicates the phosphorylated peptides. The peptide sequences are reported in Table 3.

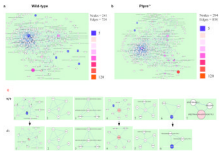

Fig. 6. The red cell signaling network topology is altered by the absence of PTPε

The sub-network of phosphorylated proteins in wild-type (+/+) and in Ptpre$^{-/-}$ (−/−) mouse red blood cells. **(a): *Wild-type*:** Proteins are represented as circles (241), interactions as edges (724). Bigger circle diameter indicates higher phosphorylation. The color scale code (scale from blue to red) also indicates degree of phosphorylation, with blue corresponding to 5 and red to 120 arbitrary units of phosphorylation, as derived from densitometric analysis of phosphorylated protein spots (see methods). (**b**) ***Ptpre*$^{-/-}$:** Proteins are represented as circles (294), interactions as edges (838). Bigger circle diameter indicates higher phosphorylation. The color scale code (scale from blue to red) also indicates the degree of phosphorylation, with blue corresponding to 5 and red to 120 arbitrary units of phosphorylation, as derived from densitometric analysis of phosphorylated protein spots (see methods).

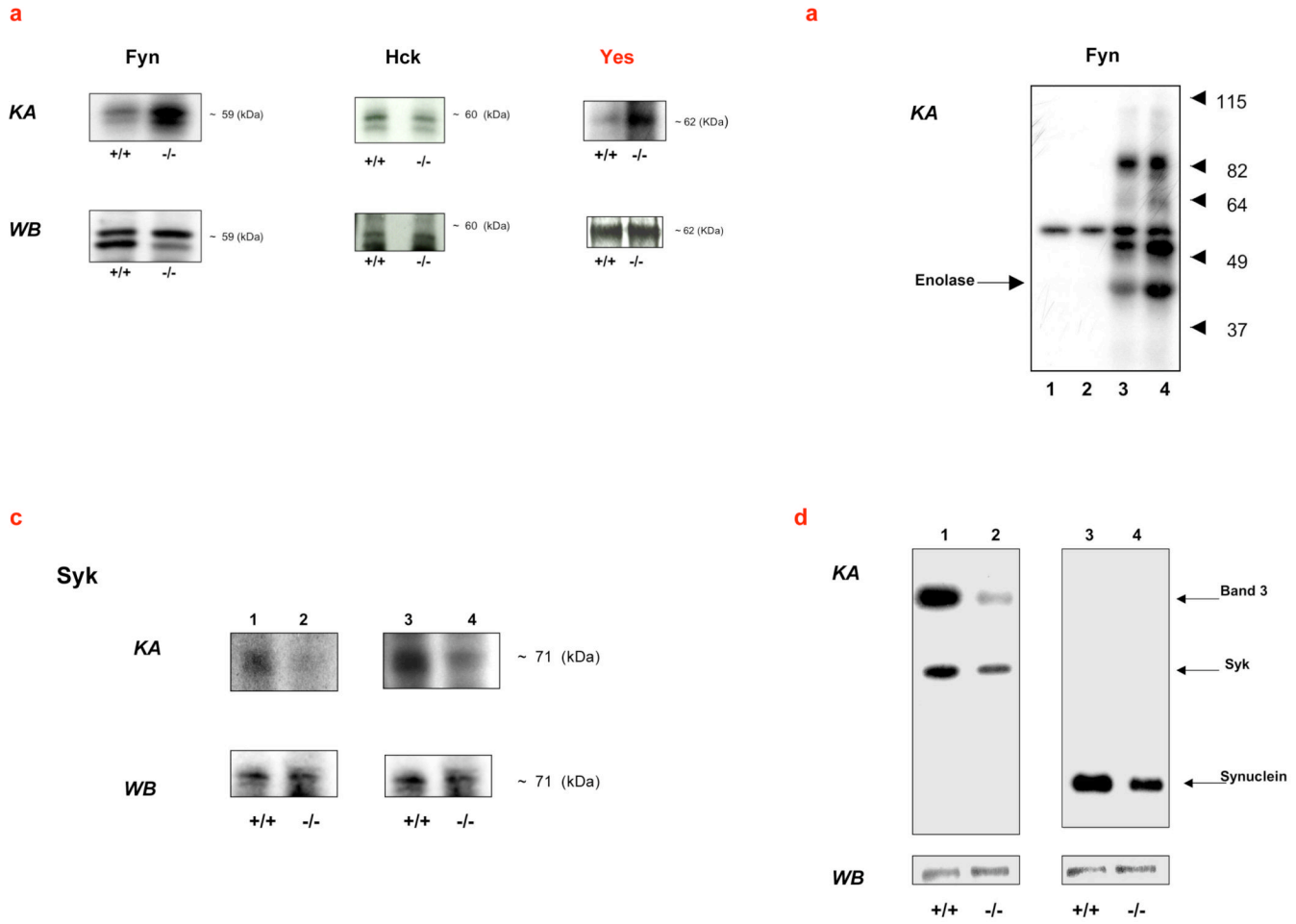

Fig. 7. Modular decomposition identified Tyr-phosphorylated sub-network and in vivo validation shows abnormal Syk kinase activity in red cells lacking PTPε

(a) Modular decomposition and identification of protein complexes in sub-network of phosphorylated proteins in wild-type (+/+) and in Ptpre$^{-/-}$ (−/−) red blood cells. Proteins are represented as circles, interactions as edges. The color scale code indicates degree of phosphorylation. Clusters were identified with Cytoscape by using the MCODE algorithm plug-in (see methods). Arrows indicate modification of complexes in wild-type *vs* knockout red cells. **(b)** Syk kinase activity in ghosts and cytosol fractions from wild-type (lane 1 and 3; +/+) and Ptpre$^{-/-}$(lane 2 and 4;−/−) mouse red cells. The immunoprecipites were subjected to *in vitro* kinase assays (*KA*) and then western-blot analysis (*WB*) with the corresponding specific antibody. The KA for the ghosts fraction required longer time of exposure (24 hours; hrs) compared to the cytosol fraction (12 hours; hrs). Shown is a representative experiment of 3 performed with similar results. **(c)** Syk kinase activity in red cells from wild-type (+/+; lane 1 and 3) and Ptpre$^{-/-}$mice (−/− lane 3 and 4) using two endogenous substrates: band 3 or synuclein in presence of γ [^{32}P] ATP (see methods). The samples were subjected to immunoblotting with anti-Syk (*WB*). The blots were analyzed by autoradiography. Shown is representative experiment of 3 performed with similar results.

TABLE 1

Hematological parameters, phophatydyl-serine positive red blood cells and red cell cation content in wild-type and Ptpre$^{-/-}$ mice

	Wild-type (*n*=9)	Ptpre$^{-/-}$ (*n*=9)	*P*
Hct (%)	45±1.7	44.3±1.2	NS
Hb (g/dL)	14.5±0.8	15.2±0.3	NS
MCV (fL)	51.2±0.33	48.8±0.9*	**0.005**
MCHC (g/dL)	27.8±0.1	29.9±0.5*	**0.004**
RDW (%)	14.1±0.4	12.8±0.5*	**0.0031**
HDW (g/dL)	1.68±0.01	1.90±0.03*	**0.014**
Retics (%)	3.3±0.1	3.8±0.2	NS
MCVr (fL)	64.4±2.9	59.1±1.3*	**0.004**
MCHCr (g/dL)	24.8±0.09	26.7±0.1*	**0.001**
RDWr (%)	16.9±2.6	13.5±1.3*	**0.0007**
HDWr (g/dL)	2.61±0.03	2.69±0.02	NS
PS-positive RBCs (%)	0.49±0.12	0.59±0.32	NS
RBCs [Na^+] (mmol/Kg Hb)	35.2±2.8	33.1±0.5	NS
RBCs [K^+] (mmol/Kg Hb)	459±22	374±28*	**0.004**

Hct: hematocrit; Hb: hemoglobin; MCV: mean cell volume; MCHC: mean cell hemoglobin concentration; RDW: red blood cell distribution width; HDW: hemoglobin distribution width; MCVr: reticulocyte mean cell volume; CHCMr; reticulocyte mean cell hemoglobin concentration; RDWr: reticulocyte cell distribution width; HDWr: reticulocyte hemoglobin distribution width; PS-positive RBCs: phosphatydyl-serine positive red blood cells. Data are presented as means ± SD (*n* of experiments).

Proteomics. Author manuscript; available in PMC 2010 December 22.

TABLE 2

List of identified proteins displaying different degrees of Tyr-phosphorylation in wild-type and Ptpre$^{-/-}$ mice

			Wild-type		Ptpre$^{-/-}$	
Spot #	**Accession No**	**Protein Description**	**Matching peptides**	**Coverage (%)**	**Matching peptides**	**Coverage (%)**
1D						
1	gi17380523	Erythroid spectrin alpha chain	-	-	19	9
2	gi2506246	Beta spectrin erythroid	-	-	17	10
3	gi81890181	Erythroid ankyrin	-	-	10	11
4	gi6755560	Erythrocyte membrane protein band 3	-	-	8	11
5	gi38570129	Erythrocyte membrane protein band 4.1	-	-	9	12
6	gi485736	Erythrocyte membrane protein band 4.2	-	-	11	16
7	gi6671509	Actin beta	-	-	7	24
8	gi40254525	tropomyosin	-	-	7	36
2D						
1	gi6755560	Erythrocyte membrane protein band 3	15	20	12	16
2	gi6671509	Actin beta	12	40	5	16
3	gi20809750	Tropomyosin 3, gamma	6	18		
4	gi81890181	Erythroid ankyrin	18	21	16	15
5	gi22477509	Erythrocyte membrane protein band 4.9	4	15	8	28
6	gi17380523	Erythroid spectrin alpha chain	15	28	7	14
7	gi3986773	Heat Shock protein-70 kDa (HSP70)	11	19	nd Ptpre−/−	
8	gi2499469	Peroxiredoxin 2	4	33	6	40
9	gi15488600	Membrane protein palmitoylated	9	32	8	30
10	gi729896	Src-family-kinase Fyn	14	30	11	33
11	gi40254525	Tropomyosin	6	32		
12	gi10125957	Peroxiredoxin 5	nd WT		8	45
13	gi38570129	Erythrocyte membrane protein band 4.1	nd WT		10	15
14	gi485736	Erythrocyte membrane protein band 4.2	nd WT		13	18
15	gi2506246	Beta spectrin erythroid	nd WT		18	9
16	gi31981690	Heat Shock protein 8 (HSP8)	nd WT		20	41

			Wild-type		Ptpre$^{-/-}$	
Spot #	**Accession No**	**Protein Description**	**Matching peptides**	**Coverage (%)**	**Matching peptides**	**Coverage (%)**
17	gi14916528	Erythroid beta adducin	nd WT		18	25
18	gi45592932	Proteosome 4 subunit beta	nd WT		5	34
19	gi809561	Gamma actin	nd WT		10	30

The corresponding bands and spots are indicated in Figure 4; nd: not detectable in either wild-type (WT) or Ptrpre$^{-/-}$;

-band not excised.

TABLE 3

Identification of tyrosine-phosphorylated residues in tropomyosin, α- spectrin and ankyrin in wild-type and Ptpre$^{-/-}$ mouse red cells

Protein name	Obsd mass	PY residues	Posphorylated Peptides	Mouse strain
Tropomyosin-3	1460.89	214	SLEAQAEKYSQK + HPO3@Y	**WT**
Spectrin alpha chain	1195.44 1275.47	984	VIALYDFEAR VIALYDFEAR + HPO3@Y	**Ptre$^{-/-}$**
Spectrin alpha chain	1857.76 1938.90	546	LIDNDHYDSENIAAIR LIDNDHYDSENIAAIR + HPO3@Y	**Ptre$^{-/-}$**
Ankyrin	2120.21	1079	SWTLPTASYILDQDFKR + 2HPO3@Y	**Ptre$^{-/-}$**

Obsd mass: observed mass; PY: tyrosine phosphorylated residues; @: phosphorylated residues; WT: wild-type mouse strain.